

Research Article

Open Access



Enhancing urban resilience in historical centers: a scenario-based approach to seismic risk and strengthening interventions

Hooman Mehralian¹, Nicola Chieffo² , Mason Moritz¹, Busra Gögen¹, Alireza Khodadadi¹, Monica Amaral Ferreira³, Carlos Sousa Oliveira³

¹School of Engineering, Department of Civil Engineering, ISISE, ARISE, University of Minho, Guimarães 4800-058, Portugal.

²Department of Engineering, School of Computing and Engineering, University of Huddersfield, Queensgate, Huddersfield HD1 3DH, UK.

³CERIS, Instituto Superior Técnico, Universidade de Lisboa, Lisbon 1049-001, Portugal.

Correspondence to: Dr. Nicola Chieffo, Department of Engineering, School of Computing and Engineering, University of Huddersfield, Queensgate, Huddersfield HD1 3DH, UK. E-mail: n.chieffo@hud.ac.uk

How to cite this article: Mehralian H, Chieffo N, Moritz M, Gögen B, Khodadadi A, Amaral Ferreira M, Oliveira CS. Enhancing urban resilience in historical centers: a scenario-based approach to seismic risk and strengthening interventions. *Dis Prev Res* 2024;3:12. <https://dx.doi.org/10.20517/dpr.2024.13>

Received: 27 Jul 2024 **First Decision:** 14 Oct 2024 **Revised:** 30 Oct 2024 **Accepted:** 15 Nov 2024 **Published:** 30 Nov 2024

Academic Editor: Jie Li **Copy Editor:** Fangling Lan **Production Editor:** Fangling Lan

Abstract

The proposed study deals with seismic vulnerability assessment and highlights the importance of evaluating urban vulnerability in historic areas. Focusing on Portugal's mainland, the case study area is located within the historical part of the Lisbon city council. The main objective of the proposed research is to evaluate the seismic vulnerability of existing unreinforced masonry residential buildings, given their prevalent nature and sensitivity to earthquake damage. This study, by providing an example of an urban-scale assessment approach, offers an overview of potential strengthening solutions and proactive risk-reduction measures in seismically-prone areas. To gather comprehensive information on the problem, a methodology was developed including site inspections integrated with remote sensing data. This combined approach highlighted the importance of conducting remote sensing with careful consideration and input from experts in building characteristics. Urban renovation works in historical centers often preserve architectural styles while altering physical structures. Without proper documentation, this revitalization can introduce errors, weakening the accuracy of seismic assessments. Expected damage scenarios were preliminarily estimated, and typological fragility curves were evaluated. Additionally, economic losses and repair costs were assessed. However, further studies are necessary to calibrate these results, particularly in terms of customizing the building typology characterization to the specific context of the Lisbon City Council.

Keywords: Vulnerability assessment, loss estimation, urban resilience, historical masonry buildings



© The Author(s) 2024. **Open Access** This article is licensed under a Creative Commons Attribution 4.0 International License (<https://creativecommons.org/licenses/by/4.0/>), which permits unrestricted use, sharing, adaptation, distribution and reproduction in any medium or format, for any purpose, even commercially, as long as you give appropriate credit to the original author(s) and the source, provide a link to the Creative Commons license, and indicate if changes were made.



INTRODUCTION

While the global perspective provides valuable insights into seismic risk mitigation, it is crucial to examine the specific conditions of Lisbon. Conducting a seismic vulnerability assessment in Lisbon is essential due to the city's rich architectural heritage and unique seismic history. The central buildings in Lisbon are classified into different types, each with distinct seismic characteristics and historical significance, such as Pre-Pombalino, Pombalino, Gaioleiro, and Placa. These construction typologies play a critical role in shaping the city's urban landscape and introduce diverse challenges for seismic resilience^[1,2].

The current research acknowledges the seismic sensitivity of each typology, influencing the risk environment in Lisbon. Pre-Pombalino buildings, lacking seismic resistance, have been repurposed post-restoration. Pombalino buildings, incorporating "Gaiola Pombalina" walls, demonstrate strength with a blend of traditional and advanced seismic techniques. Gaioleiro buildings adapt to the terrain with timber frames and flexible structures. Placa buildings, built between 1930 and 1960, despite criticisms due to the increased weight, use masonry as the main structural material, with reinforced concrete (RC) slabs in humid zones of the floor, and later in the complete floor^[2].

By evaluating the seismic vulnerability of masonry residential buildings in the historic center of Lisbon, and considering the nuances of each construction typology, the research aims to provide insights into tailored risk mitigation strategies. Recognizing the seismic performance variations among these typologies is fundamental for developing interventions that align with the specific needs and challenges posed by Lisbon's diverse architectural landscape.

The importance of mitigating seismic risk in historic city centers with aging building stock has grown due to catastrophic earthquakes, such as Haiti^[3], Japan's Tohoku^[4], and recent events in Turkey and Syria^[5], causing widespread casualties, economic costs, and irreparable heritage losses. Statistics from 1992 to 2012 reveal the extensive impact of natural calamities, with earthquakes emerging as the most devastating, contributing to 26% of economic losses since 1900 and causing 40% of deaths from natural catastrophes since 1960, particularly affecting masonry buildings. These findings highlight the long-term effects of seismic disasters on both human life and economic stability^[6]. Seismic evaluations face challenges due to time and cost, leading to territorial seismic vulnerability assessments. These assessments use simplified methodologies to reduce costs while still providing significant results. Urban risk assessment has progressed for specific natural disasters, but there is a lack of integration for cumulative effects of future risks in urban management practices. Authorities should adopt proactive risk-reduction initiatives, including a comprehensive risk assessment methodology, to gauge the impact of natural disasters in urban settings^[7]. In the global context, various studies have contributed to the understanding and mitigation of seismic risks in historic city centers with aging building stocks. Research conducted worldwide has explored different methodologies, strategies, and technologies for large-scale seismic assessments. It is essential to review and incorporate insights from these studies to enrich the comprehensiveness of our research. This comparative analysis will provide a broader perspective on the challenges and solutions associated with seismic risk mitigation in urban settings^[8-12].

Seismic risk evaluation of urban areas involves assessing the probability of seismic events of certain intensities occurring at specific sites within a given timeframe. A critical part of this evaluation is assessing the vulnerability of the building stock, as it is the main factor that can be engineered to mitigate risk. Given the vast amount of data needed for such assessments, simpler methodologies are often preferred. These methods can be empirical, based on observed damage from past earthquakes, or analytical, involving models of representative buildings to predict responses to seismic activities.

Empirical methods are well-suited for historic city centers with extensive earthquake records, utilizing damage probability matrices, vulnerability index methods, continuous vulnerability curves, or screening methods^[7,9]. Analytical methods are more detailed and transparent, suitable for cases with well-documented construction details, and allow for calibration of specific building and hazard characteristics^[10]. Heuristic methods, which rely on expert judgment, are useful for generating vulnerability curves for well-defined structural classes^[13]. Hybrid approaches combine empirical data and expert judgment to address the limitations of other methods, offering a comprehensive assessment by integrating multiple information sources^[14]. Consequently, relevant examples of hybrid approaches include the macroseismic method and specific vulnerability assessments for façade walls, combining empirical and analytical results. This article employs a hybrid approach to leverage both empirical data and expert judgment, providing a balanced and comprehensive assessment of seismic vulnerability for the historic center of Lisbon.

The seismic hazard on Portugal's mainland varies from moderate to high^[15], with a concentrated level of risk in the southwest, primarily due to powerful offshore events. Additionally, the Lower Tagus Valley area, located in Lisbon, experiences heightened vulnerability. Historical earthquakes, such as the 1722-M6.0 Algarve, 1755-M8.5 Lisbon, 1909 M6.3 Benavente, and 1969 M7.8 Algarve events, have resulted in significant damage to the country's building stock^[15-18]. As depicted in the work of Silva *et al.*, a probabilistic seismic risk analysis for the country was evaluated, estimating an average annual loss equivalent to 0.29% of the national gross domestic product, GDP^[19]. According to the above-introduced research work^[7], masonry buildings contribute significantly to the economic earthquake risk, representing 79% of it, while constituting approximately 51.5% of the total building stock^[20]. Several empirical and analytical studies have highlighted that the above-mentioned building type increased seismic sensitivity^[21-26]. This vulnerability primarily stems from factors such as low tensile strength, high specific weight, inadequate wall-to-wall and wall-to-slab connections, structural irregularities in both height and plan and a deficiency in maintenance. This study aims to propose a seismic vulnerability assessment methodology for the historic center of Lisbon. In the initial phase, data relevant to the specific study site were gathered and examined. Parameters, such as building materials, construction methods, and historical significance, for different building types were then defined^[27]. Subsequently, a vulnerability index was assigned to each building to assess its susceptibility to earthquakes^[28-30]. Statistical methods were employed to create curves indicating the likelihood of damage in various seismic scenarios. After evaluating these scenarios, potential losses were estimated for the historic center of Lisbon.

The primary focus of the study was the assessment of masonry residential buildings, predominantly made with stone or brick, which are notorious for their brittleness during seismic events. The analysis considered various factors such as construction methods, material changes, and emergency modifications, as these interactions significantly influence a building's vulnerability. Surveys, assisted by tools such as Google Earth, were conducted to inspect buildings and assign plausible vulnerability parameters to each one. Based on this vulnerability index, expected damage scenarios were developed for a seismic event with a return period of 475 years. Fragility curves played an important role in estimating potential damage scenarios by showing how likely specific damage is at different levels of seismic intensity.

To determine the probabilities of collapse and functional deficits, the study proposed by Bramerini *et al.* was considered since it provides several related factors to estimate building losses after minor or moderate seismic actions^[31]. Transitioning to economic considerations, damage assessments were carried out, taking into account material, labor, and additional costs. The evaluations encompassed both the replacement cost

of damaged buildings and the cost of retrofitting the affected area. Finally, a resilience index was presented to offer an overview of the current condition of the buildings. The research was conducted in collaboration with the ReSist Program^[32-34], a municipal initiative aimed at assessing the city's seismic vulnerability. The program encompasses management plans, educational campaigns, site inspections, and criteria for prioritizing interventions. The purpose is to complement these efforts by incorporating a methodology for large-scale vulnerability assessment and providing intervention recommendations.

THE CASE STUDY AREA

Historic seismicity of Lisbon

Portugal finds itself in a seismic hotspot due to its proximity to the Eurasian and African Plates. This geological reality affected the region with a series of destructive earthquakes over the centuries. The country's hazard level is classified as "high" due to the upcoming potential for extremely large offshore earthquakes, and "moderate" due to the potential of significant onshore seismic activity^[35].

Lisbon stands proudly on the right bank of the Tagus River, boasting an expansive area of 100 km². This area comprises 24 parishes, each contributing to Lisbon's cultural and historical heritage^[36]. However, the city's resilience has been shaped over the centuries by the relentless force of destructive earthquakes. The first significant seismic event occurred in 1531, leading to the tragic collapse of 1,500 houses and an alarming toll of 30,000 casualties. The effect of the devastating event persisted, with another earthquake in 1579 causing the disappearance of three streets, leaving a permanent mark on the city's landscape. The turning point for Lisbon arrived in the aftermath of a devastating earthquake in 1755. The city emerged from the ruins and started a restoration effort that symbolized the beginning of the modern period^[37]. The buildings were endowed with unique features, including an antiseismic wooden structure known as the Pombaline cage - Gaiola Pombalina - which could be considered the genesis of seismic engineering in Europe. Lisbon faces a substantial earthquake risk because of its location in a seismically active region, especially close to the Fault of Tagus Lower Valley. Nowadays, according to the Portuguese National Annex^[38], the seismicity level in the Lisbon Metropolitan Area (LMA) can reach a maximum intensity of IX and X. The hazard level for Lisbon is significant, ranging from 0.2 to 0.3 g for a 475-year return period^[39]. [Table 1](#) presents a summary of Portugal's earthquake history by combining historical and instrumental data. Before the instrumental era, some magnitude information was missing due to the lack of earthquake stations. However, they are described by Modified Mercalli Intensity (MMI) as mainly greater than or equal to an intensity of IX. At the beginning of the 20th century, instrumental measurements began to be used, and information regarding earthquakes, such as time, location, magnitude, and depth, was recorded respectively. As introduced in the above-mentioned [Table 1](#), the most recent severe earthquake, with a moment magnitude (M_w) of 7.8, occurred in 1969. This seismic event was not only felt in the epicenter region but also had significant impacts on neighboring countries. The earthquake triggered a tsunami, adding to the overall impact and demonstrating the far-reaching consequences of this seismic event^[40].

Identification of prevalent structural typologies and damages

Lisbon's architectural history is rich and diverse, influenced by Gothic, Renaissance, Baroque, Rococo, and Neoclassical styles. Before the 1755 earthquake, the city featured a mix of Gothic, Renaissance, and Baroque elements, with stone or masonry construction, ornate facades, and narrow streets.

Post-earthquake, led by the Marquis of Pombal, reconstruction efforts emphasized durable materials, resulting in four or five-story structures with wider streets and earthquake-resistant features^[41].

Table 1. Historical and instrumental seismic records of Portugal

Year	Location	Magnitude M_w	Depth km	MMI	Notes	Deaths
210 BCE	Cape St. Vincent	-	-	-	Possible tsunami	
60 BCE	coast of Portugal	8.5	-	IX	Tsunami	
382	Cape St. Vincent	7.5	-	-	Tsunami	
1344	Lisbon	-	-	-	-	
1358	Lisbon	-	-	X	Severe damage in Seville and Lisbon	
1531	Lisbon	7.7	-	-	At least 1,500 houses were destroyed. Violent earthquake felt in Africa. A large tsunami was reported	30,000
1551	Lisbon	-	-	-	About 200 houses were destroyed	2,000
1587	Loulé	-	-	X	-	170
1597	Monte Santo	-	-	IX	-	
1722	Tavira, Algarve	-	-	X	At least 27 homes collapsed in Tavira. Albufeira, Loule, Lagoa, and Faro also reported damage	
1755	Atlantic Ocean	8.5-9.0	-	XI	Lisbon was almost destroyed by the earthquake and subsequent conflagrations. A large tsunami with a maximum height of 18.3 meters	20,000-40,000
1756	Lisbon	-	-	-	-	
1761	Atlantic Ocean	8.5	-	IX	Lasted 5 min	
1816	North Atlantic	8.3-8.9	-	VII	Damage and deaths in Ovar. One death in Lisbon. Felt in Spain, the Netherlands, and the Azores Islands	13+
1858	Setúbal	7.1	-	X	605 homes were destroyed	8
1909	Santarem District	6.0	10	X	Salvaterra de Magos and Benavente were partially destroyed	60
1969	Gulf of Cádiz	7.8	22	VII	Deaths in Morocco, Portugal, and Spain. Tsunami observed	25

The city's central buildings are classified into different types, i.e., Pre-Pombalino, Pombalino, Gaioleiro, and Placa [Figure 1]. Pre-Pombalino buildings lacked seismic resistance due to their construction methods and materials. However, after restoration, these structures served various purposes, showcasing their adaptability and functionality. Pombalino buildings, crafted in the aftermath of earthquakes, showcase robustness through the incorporation of "Gaiola Pombalina" walls. These walls ingeniously blend traditional wooden construction techniques with advanced seismic principles, highlighting a design that prioritizes earthquake resistance and structural stability. Gaioleiro buildings in the historic center are designed to match and work well with the natural features of the land. Using timber frames and flexible structures, these buildings adapt to the terrain by adjusting to any shifts or settling in the ground. In essence, they are smartly crafted to fit in harmoniously with their surroundings. Placa buildings incorporate RC frame elements, which, despite being durable and cost-effective, face criticism for their architectural quality. Critics argue that these structures lack aesthetic appeal or distinctive design features, expressing concerns about their visual uniqueness. Despite their proven durability and cost efficiency, the buildings are challenged for not meeting certain standards in terms of architectural creativity and overall attractiveness. Recent efforts aim to renovate and upgrade Placa structures while preserving their architectural heritage in Lisbon^[1,2].



Figure 1. Typology of Portugal's historic masonry buildings: Pre-Pombalino, Pombalino, Gaioleiro, and Placa. It highlights the characteristics and structural features of each typology, emphasizing their historical significance and variations in construction methods.

The historic multicultural center of Lisbon, Mouraria, is primarily situated along Rua da Palma and Avenida Almirante Reis [Figure 2].

This area, central to the Lisbon city council, served as a primary focus of the study. Approximately 300 mixed-use masonry buildings within the case study area were identified and mapped in ArcGIS for geospatial visualization. The methodology started with systematically collecting data on building typologies, facilitating a refined analysis of structural behavior, material characteristics, and necessary assumptions.

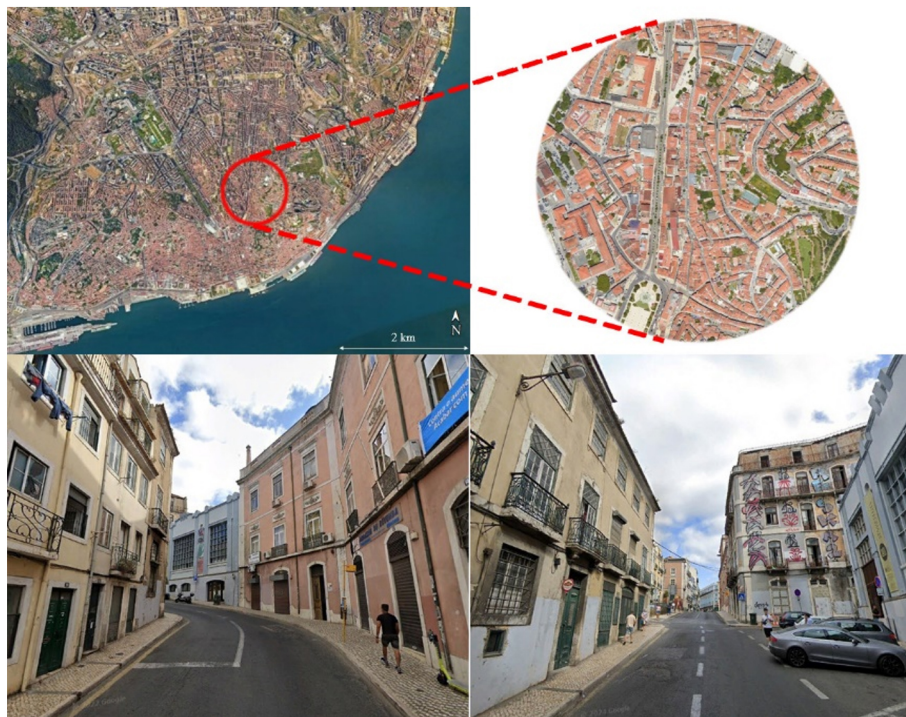
Structural units (SUs) were initially inspected remotely using Google Street View imagery and facade and opening area analysis^[42,43], supported by building drawings provided by the Municipality of Lisbon as essential input data. This approach integrates preliminary remote evaluations with detailed on-site inspections and web-mapping assessments, providing a comprehensive understanding of the main features of the building stock and enabling the method's effective application.

The methodology builds on established practices with specific adaptations for Lisbon's historic center. This study introduces refinements tailored to this context, which have not been published previously, ensuring that both the structural and cultural aspects of Lisbon's historic masonry buildings are appropriately addressed.

In the literature, two distinct typological classifications were developed. The first followed the model proposed by Bernardo *et al.* for the LMA; however, the study area differs significantly from the LMA^[44]. Bernardo *et al.* also emphasized the need for further research to reduce the existing variability in these models, including the assignment of typologies and their respective vulnerabilities^[44]. The second classification adopts the Risk-EU classification system, a European standard for buildings that correspond to the European Macroseismic Scale 1998 (EMS-98) [Table 2]^[45]. The alignment between LMA and Risk-EU typologies was assumed by using the masonry building feature comparison matrix^[29], which identifies common construction materials and features among 60,000 surveyed masonry buildings. Table 2 provides a direct conversion from a global to a local typology scale based on material similarities.

Table 2. Risk-EU typological classification and similarities in the LMA region

	Typologies according to the risk-EU method	Local typology in LMA
M1	Rubble stone	Pre-Pombalino
M2	Adobe	-
M3	Simple stone	Pre-Pombalino
M4	Massive stone	Pombalino
M5	URM (Old bricks)	Pombalino
		Gaioleiro
M6	URM with RC floors	Placa
M7	Reinforced/Confined masonry	RCM

**Figure 2.** Study area: Mouraria, Metropolitan area of Lisbon^[42].

The construction typologies showed significant variation, including multiple local architectural types incorporating into three or more EMS-98 typologies. The predominant structural typology among masonry buildings consists of rubble masonry with wooden floors (M1), constituting 57% of the surveyed buildings. The second most prevalent typology is unreinforced brick masonry with wood floors (M5), accounting for 37% of the investigated sample. The third most common typology is unreinforced brick masonry with RC floors (M6), representing 6% of the examined compounds. However, only one surveyed building was identified as a confined masonry structure [Figure 3A and B]. Moreover, the distribution of the buildings investigated in the area based on the number of stories is depicted in Figure 3C. Vulnerability models aim to establish a link between hazards and structural damage, necessitating a standardized classification for observed damage. EMS-98^[45] proposes discrete damage levels, ranging from negligible slight damage to total or near-total collapse. Preliminary rapid screenings of SUs enabled the evaluation of the existing damage condition of each building. The survey activity facilitated the detection of damages, enabling the identification of the propagation of damage. The observed damages were then correlated with EMS-98

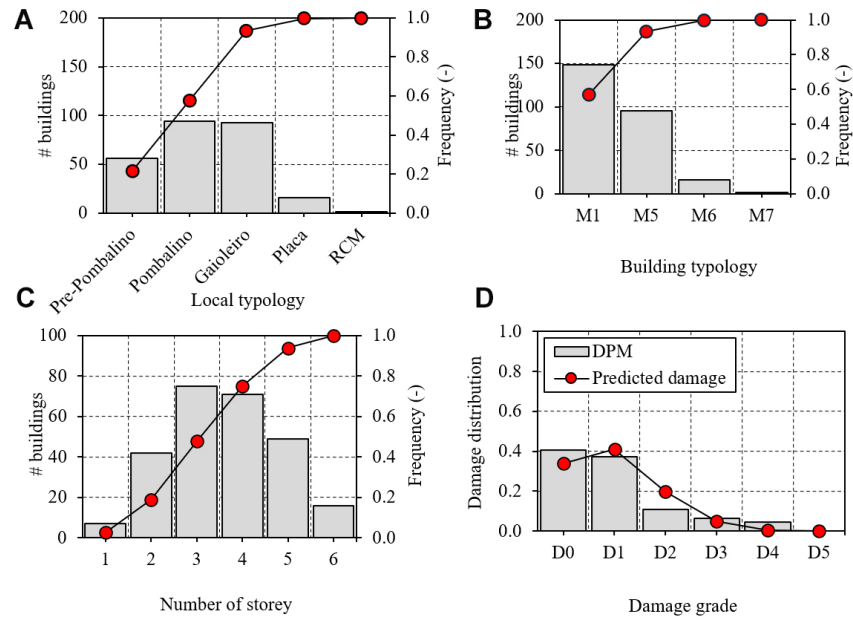


Figure 3. Statistical data on the 300 inspected masonry buildings. (A) local typologies; (B) building typologies; (C) number of stories; (D) damage grades.

thresholds, achieved through the development of a Damage Probability Matrix (DPM), which is produced based on the weighted average of observed damages according to

$$\begin{cases} p_k = \frac{5!}{k!(5-k)!} \cdot \left(\frac{\mu_D}{5}\right)^k \cdot \left(1 - \frac{\mu_D}{5}\right)^{5-k} \\ \mu_D = \sum_{k=1}^5 p_k \cdot k \end{cases} \quad (1)$$

where p_k is the probability of exactly k buildings exhibiting a specific level of damage and μ_D is the average damage level across all buildings. Figures 3D and 4A depict the expected damage levels for a seismic event with a return period of 475 years, consistent with standard practices for seismic assessments in Lisbon. The average damage μ_D is influenced by the intensity of the seismic action, which is based on a representative seismic hazard curve for the region. This correlation between seismic intensity and expected damage is essential for the analysis.

The parameter k serves as a weighted factor within the DPM, and it utilized values consistent with those proposed in the literature for the types of masonry buildings prevalent in Lisbon. These values reflect empirical data from past seismic events and will be explicitly detailed in the revised manuscript to ensure clarity. The resulting DPM, presented in Figure 3D, indicates a weighted average damage of $\mu_D = 0.96$. It shows that 41% of the analyzed buildings have no damage (D0), 37% have slight damage (D1), 11% have moderate damage (D2), 7% have substantial damage (D3), and 5% are near collapse (D4). Fortunately, for the investigated area, no building reaches the damage threshold D5 (collapse). Furthermore, the results of the case study were processed in the ArcGIS environment^[43], as shown in Figure 4.

Site inspection

In pursuit of a comprehensive understanding of the damaged state and actual condition of buildings within the LMA, a thorough site inspection was carried out. The municipality granted permission for access to a

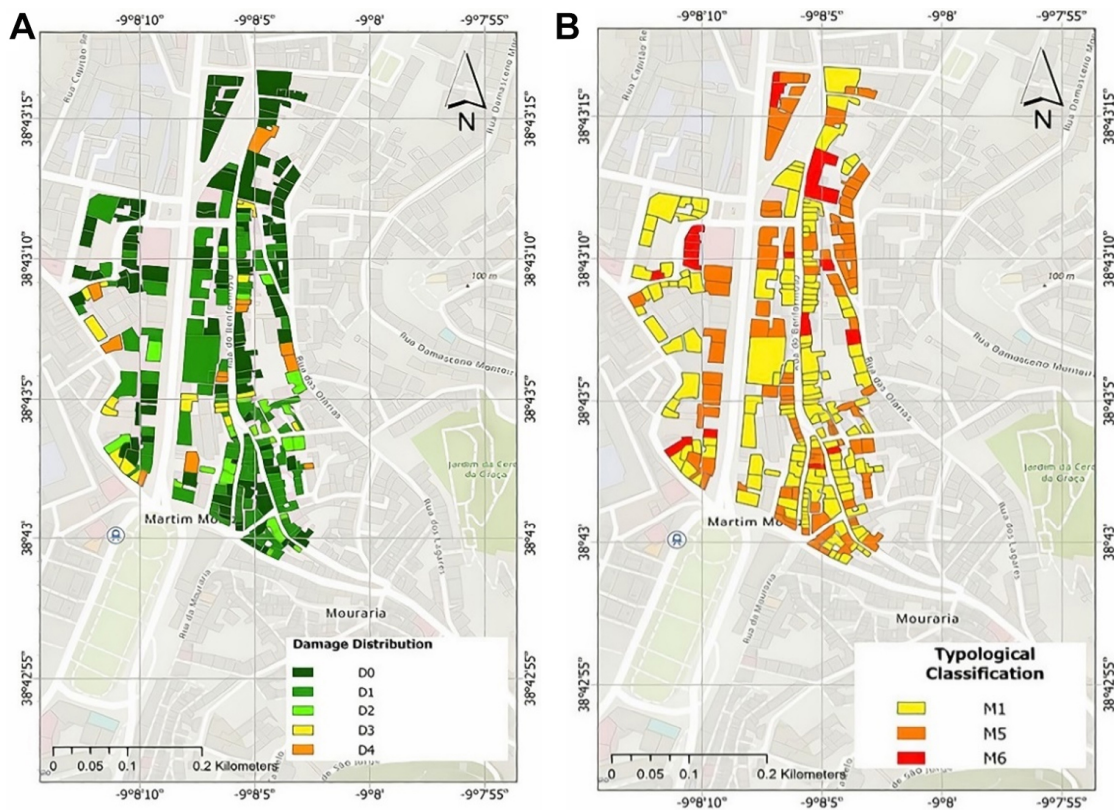


Figure 4. (A) damage grades for the investigated Lisbon Metropolitan Area (LMA). and (B) Building typologies.

few buildings, enabling a detailed examination. To systematically capture relevant information, a checklist was meticulously devised, serving as the basis for generating a comprehensive database for the examined building. The checklist incorporated fields for each parameter and sub-parameter of interest, facilitating a nuanced evaluation. The intention behind the survey activity was two-fold: first, to overcome the limitations of remote assessments by conducting a hands-on inspection, and second, to use the checklist-based methodology to generate a database that could validate assumptions made during the initial phases. The findings from the inspection were significant, indicating that the current state of the structures is notably worse than initially estimated. This finding underscores the urgent need for immediate interventions to ensure the ongoing functionality of these buildings. The inclusion of specific structural details, such as foundation integrity and material conditions, highlights the seriousness of the situation and calls for prompt, targeted actions [Figure 5]. Horizontal structures made with RC are typically considered rigid in-plane.

However, following certain events, increased levels of damage have been observed, rendering the upper floors unsafe for human occupancy. Wooden floors have been particularly affected by issues such as dry rot and water damage. The weaknesses in these floor systems pose a significant risk, which is exacerbated by events such as earthquakes that can further deteriorate the damage. The challenges in the structure are further complicated by the presence of dry rot and water damage on wooden floors. If these issues are not promptly addressed, they not only compromise the safety of occupants but also necessitate extensive repairs to restore the structural integrity of the building. To illustrate these concerns, Figures 5 and 6 provide visual examples, highlighting the urgent need for thorough assessments and targeted interventions to address the current conditions of floors and other critical components. For example, in Figure 5, seams and cracks were

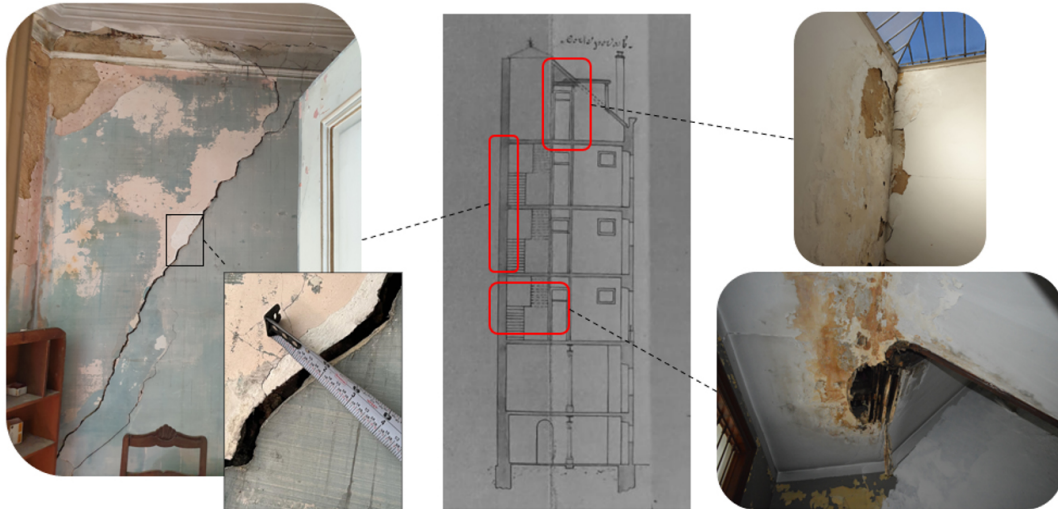


Figure 5. On-site inspection: deterioration of an example building.



Figure 6. Severe situations and deteriorated parts: Interior wall (A), roof (B), and floor (C).

observed in the walls, which were as large as 3-5 cm, indicating significant structural distress. These fissures not only compromise the aesthetic integrity of the building but also serve as critical indicators of underlying issues that may affect overall stability. Furthermore, water leakage was noted, penetrating the walls and leading to decay in the surrounding materials. This decay not only weakens the structural components but also creates a conducive environment for mold growth, which poses health risks to occupants. The cumulative effect of these damages ultimately resulted in the collapse and destruction of key elements of the main structure.

Figure 6 demonstrates the devastating situation and underscores the need for urgent intervention. The visual representation in this figure, such as rotten wooden walls and ceiling, highlights the severity of the damage, showcasing areas where structural integrity has been compromised, further emphasizing the immediate requirement for thorough assessments and remedial actions.

VULNERABILITY ASSESSMENT OF MASONRY AGGREGATES

Index-based vulnerability approach

The expected vulnerability is assessed through various empirical methodologies^[27-30]. These methods utilize specific survey forms that outline relevant typological, structural, and material criteria, enabling a comprehensive evaluation of the vulnerability level. Primarily, these procedures rely on the Vulnerability

Index Method (VIM) to derive a synthetic parameter reflecting the level of intrinsic vulnerability achieved by a particular structural system^[10,46-48]. In the context of the LMA, the VIM is applied to assess historic masonry buildings. The survey form, which has been widely used across Europe^[30,48-50], encompasses 15 parameters considering the interaction between SUs that constitute the masonry aggregate. The adopted survey form is depicted in [Table 3](#).

Concerning the presented information, [Table 3](#) categorizes factors into four groups (A, B, C, D), signifying varying vulnerability levels for a building. These groupings illustrate how individual components influence the overall vulnerability of the structure. Each component is assigned a specific score (S_i), and higher scores correspond to higher assessed classes (ranging from Class A, the best, to Class D, the least favorable). Additionally, there is a variable weight (W_i) ranging from 0.25 to 1.50. Notably, the suggested weights and scores underwent meticulous calibration and validation through non-linear numerical analyses^[10]. These analyses were conducted on real case study masonry buildings with different vertical structures and materials, as outlined in^[30]. The vulnerability evaluation for the urban compound was performed using Python Code^[51]. Functions were crafted to leverage the Pandas data analysis library, facilitating the reading of an Excel database.

The code has been made publicly available on github.com^[52] for general use, enabling anyone to implement it for seismic vulnerability assessments of historic structures. After grading and associating parameters with their respective scores, the vulnerability index (I_v) was assessed for each SU. The evaluation involves the weighted sum of the assigned scores and their corresponding weights, as given in:

$$I_v = \sum_{i=1}^{15} S_i \cdot W_i \quad (2)$$

Subsequently, the vulnerability index value (I_v) is typically normalized within the range [0 to 1], denoted by the notation V_i , as expressed below:

$$V_i = \left[\frac{I_v - \sum_{i=1}^{15} S_{min} \cdot W_i}{|\sum_{i=1}^{15} [(S_{max} \cdot W_i) - (S_{min} \cdot W_i)]|} \right] \quad (3)$$

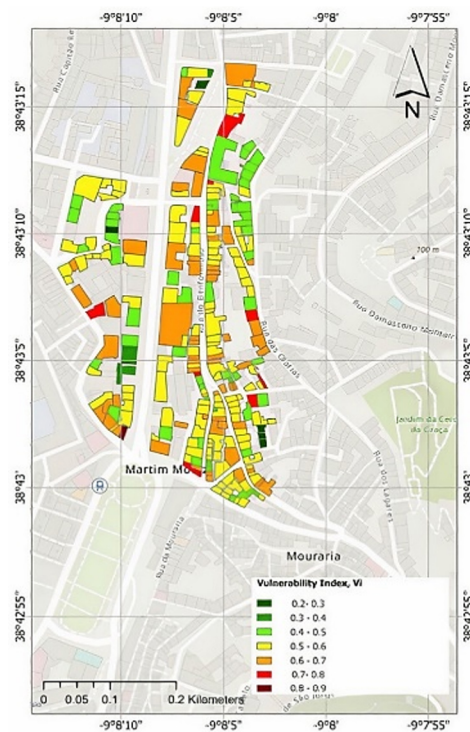
Furthermore, the vulnerability index distribution for the case study of the LMA was processed in the ArcGIS environment^[43] as shown in [Figure 7](#). The results of the vulnerability index method show that 70% of the evaluated building stock is associated with a medium-level vulnerability index ($0.4 < V_i \leq 0.6$), 26% with a medium-high vulnerability index ($0.6 < V_i \leq 0.8$), 0.4% with a high vulnerability index ($0.8 < V_i$), and 3% with a low vulnerability index ($V_i \leq 0.4$).

The analysis of collected data uses the macroseismic approach, utilizing the methodology proposed by Lagomarsino and Giovanazzi^[28]. This approach is a robust qualitative method for risk assessment, directly calibrated through post-earthquake damage data. It incorporates previously assessed vulnerability indices (V_i) and a ductility index (Q), assigned a value of 2.3, which has been observed to represent buildings not specifically designed for ductile behavior^[29]. Vulnerability curves were then generated to qualitatively assess expected damage at different levels of macroseismic intensity (MSI) using:

$$\mu_D = 2.5 \cdot \left[1 + \tanh \left(\frac{I + 6.25 \cdot V_i - 13.1}{Q} \right) \right] \quad (4)$$

Table 3. Adopted vulnerability form for structural masonry aggregates

Parameters	Class score, S_i				Weight, W_i
	A	B	C	D	
1. Organization of vertical structures	0	5	20	45	1.0
2. Nature of vertical structures	0	5	25	45	0.25
3. Location of the building and type of foundation	0	5	25	45	0.75
4. Distribution of plan-resisting elements	0	5	25	45	1.5
5. In-plane regularity	0	5	25	45	0.5
6. Vertical regularity	0	5	25	45	0.8
7. Type of floor	0	5	25	45	0.8
8. Roofing	0	15	25	45	1.0
9. Details	0	0	25	45	0.25
10. Physical conditions	0	5	25	45	1.0
11. Presence of adjacent buildings with different height	-20	0	15	45	1.0
12. Position of the building in the aggregate	-45	-25	-15	0	1.5
13. Number of staggered floors	0	15	25	45	0.5
14. Structural or typological heterogeneity among S.U	-15	-10	0	45	1.2
15. Percentage difference of opening areas among adjacent facades	-20	0	25	45	1.0

**Figure 7.** Geospatial mapping of vulnerability indices.

The curves are depicted in Figure 8, accounting for the relation between the mean damage grade (μ_D) and MSI based on the EMS-98 damage grades ranging from 0 to 5. Each building typology (M1, M5, M6, M7) is characterized by a specific mean vulnerability index of the building class and standard deviation (σ). Moreover, the curves are plotted considering up to \pm two standard deviations, σ , to statistical-related damage within upper and lower bounds for building stock.

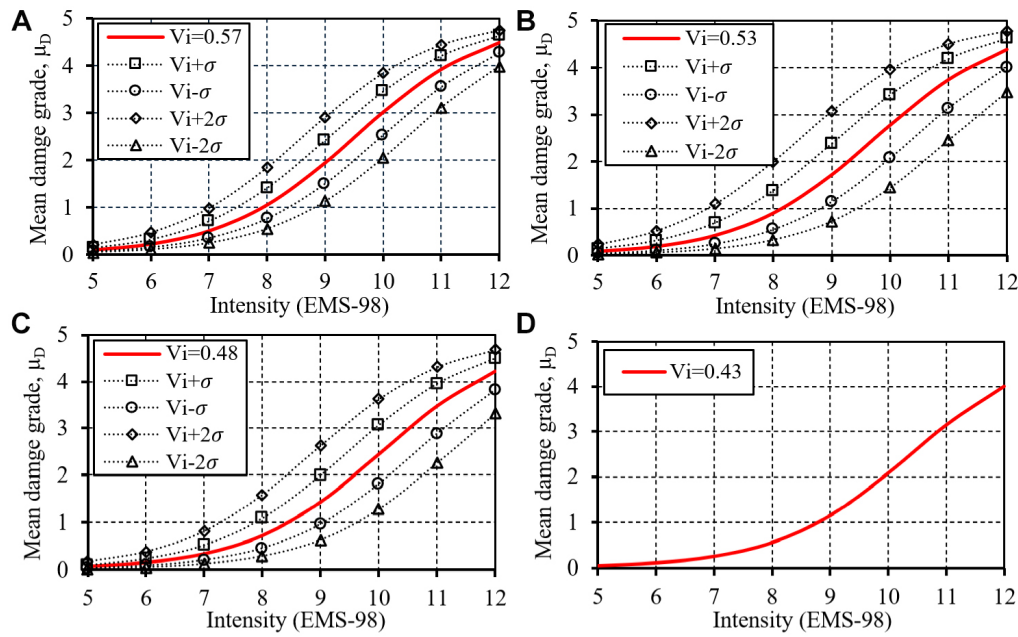


Figure 8. Mean damage curves for typologies: (A) M1; (B) M5; (C) M6; and (D) M7.

For instance, [Figure 8A](#) illustrates the mean damage grade (μ_D) for the M1 typology, which primarily consists of Rubble Stone buildings and includes some Pre-Pombalino structures, across various intensity levels. This figure also features four additional curves representing \pm two standard deviations. Conversely, in [Figure 8D](#), the M7 typology (Reinforced/Confined Masonry or RCM) lacks standard deviation curves. This is because there is only one building of that typology, resulting in a single graph without the additional standard deviation curves. Moreover, by comparing the mean damage grade (μ_D) calculated in this study with the corresponding one proposed by Oliveira^[53] for Portuguese building typologies (see [Figure 9](#)), it was observed that in the proposed study, the vulnerability indices vary between 0.57 and 0.43 for typologies M1 to M7, respectively, while Oliveira considers the mean values to range from 0.77 to 0.54 for typologies M1 to M7, respectively. Thus, from the obtained results, the proposed approach (red line) provides mean percentage differences of 30% lower than Oliveira’s^[53], which can be attributed to the use of different approaches for calculating the vulnerability parameters for masonry aggregates. Additionally, Oliveira’s proposal may take a more conservative approach, assuming a higher index for the examined buildings.

FRAGILITY CURVES

The macroseismic methodology has restricted applicability as it is assessed based on MSI, a measure typically unrelated to a suitable intensity measure for a seismic scenario based on Peak Ground Acceleration (PGA). Lagomarsino *et al.* suggest a correlation between MSI and PGA^[29], incorporating the uncertainties estimated in the correlations presented in^[28], which were computed for diverse urban centers and seismic events. The formulation used to generate the fragility curves for the case study typologies was calculated as follows:

$$\log(PGA) = a \cdot I + b \tag{5}$$

That can be converted as follows:

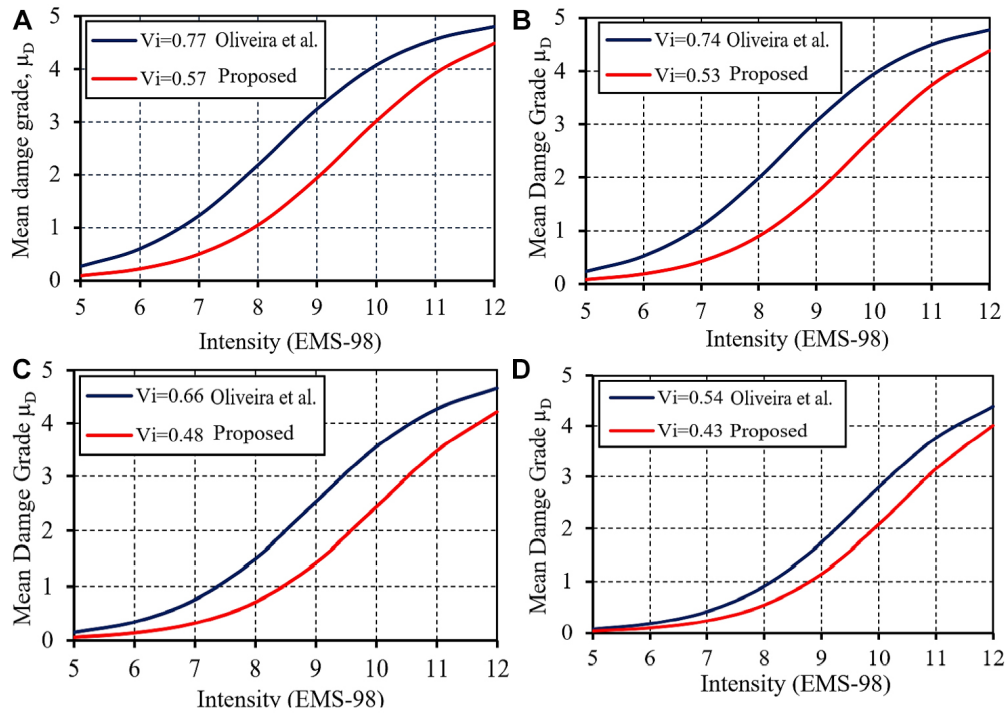


Figure 9. Comparison between the estimated damage curves and the Oliveira^[53] for (A) M1; (B) M5; (C) M6; and (D) M7 typologies.

$$\log(PGA) = c_1 \cdot I - c_2 \quad (6)$$

where c_1 and c_2 represent statistical coefficients equal to 0.602 and 7.073, respectively^[48]. The variable I denotes the MSI determined using the EMS-98 scale.

As a result, fragility curves were developed employing the binomial distribution function, which estimates the likelihood of damage based on the average damage grade, μ_D . Thus, utilizing Equation (7), the cumulative mass function was calculated to derive the fragility functions for the examined masonry typologies within the Lisbon Historical Center and the results are summarized in Figure 10.

$$P(D_i \geq D_k | I) = \sum_{k=1}^5 p_k \quad (7)$$

where the variables are defined as follows: (i) D_i : the actual damage level of a building or SU within a typology, as determined by the EMS-98 classification; (ii) D_k : a threshold damage level, representing the minimum damage level being assessed for probability; (iii) p_k : the probability of a building reaching or exceeding damage level D_k , given the MSI I . Equation (7) calculates the probability of observing a damage level D_i equals to or is greater than D_k as a cumulative function. The summation is indeed taken from 1 to 5, corresponding to discrete damage levels from D1 to D5, as specified in the EMS-98 scale.

The provided scenario illustrates the relationship between damage grades (D0 to D5) and PGA/intensities for each typology. Notably, for lower intensities, the probability of attaining the lowest damage grade is the highest, while the probability of experiencing the highest damage grade is the lowest. This indicates a lower likelihood of damage occurrence at lower intensities. In the first typology (Rubble Masonry with

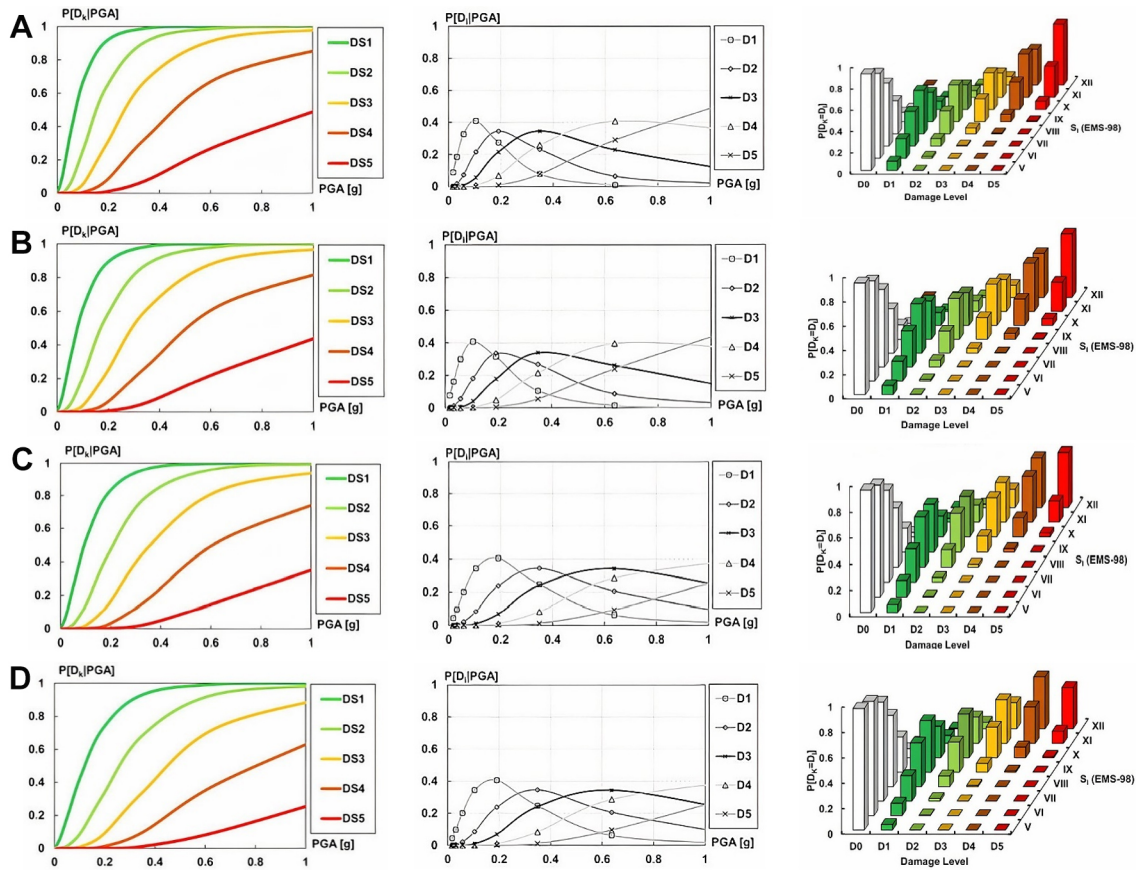


Figure 10. Fragility curves and DPM distribution for examined building typologies. (A) Rubble masonry, $V_{l,mean} = 0.57$; (B) URM with wood floors, $V_{l,mean} = 0.53$; (C) URM with RC floors, $V_{l,mean} = 0.48$; (D) Reinforced/Confined masonry, $V_{l,mean} = 0.43$.

$V_{l,mean} = 0.57$) for the intensity of V, the probability of attaining the lowest damage grade, D0, is almost 90%, whereas the probability of D5 is nearly zero.

Conversely, as intensity levels increase towards XII, the probability of a higher damage grade also grows. For example, again, in the first typology, the probability of attaining D0 in intensity XII is near zero, while that of experiencing the highest damage grade, D5, is 58%. This suggests a higher susceptibility to severe damage or devastation at higher intensity levels. It is important to note that while the D0 curves are not plotted in Figure 10, the probability of no damage (D0) is implicitly represented in the overall distribution of damage states, ensuring a comprehensive understanding of how damage probabilities relate to seismic intensities.

DAMAGE SCENARIOS

The research conducted by Lantada *et al.* has been tailored to the specific study region to characterize its seismic activity and anticipate damage scenarios over a 500-year return period^[54]. The choice of the earthquake with a 500-year return period is standard, representing MSI with a 10% probability of occurring within 50 years. This earthquake, recognized for its specific attributes, is widely utilized in seismic design and risk assessment and is typically defined in seismic regulations^[54]. This adaptation is based on the seismic hazard analysis (PSHA) results obtained by Vilanova and Fonseca^[15]. They assessed the peak ground acceleration (PGA) values for Portugal, estimating them to fall within the range of 0.05 to 0.20 g for a 500-year return period. Lantada *et al.* introduced formulations connecting ground acceleration with both

MSI and earthquake return periods^[54]. Subsequently, the resulting relationship, given in Equation (8), establishes a clear link between ground acceleration and intensity levels for various return periods. The obtained results affirm the reliability and align with the conclusions drawn by Vilanova and Fonseca^[15]. Consequently, the estimated damage scenarios are evaluated for the 500-year return period, as illustrated in [Figure 11](#). The MSI (IM) scale is used because it is related to the parameters utilized to understand the damage analysis, providing a clearer framework for assessing building vulnerability.

$$\log_{10} a_b = 0.30103 \cdot I - 0.2321 \quad (8)$$

$$a_b|_{PR=t} = a_b|_{PR=500} \left[\frac{t}{500} \right]^{0.37} \quad (9)$$

The subscript k , associated with the damage D , represents the damage thresholds ranging from 0 to 5, as follows: D0: no damage, D1 (slight): thin cracks in a few walls and minor plaster detachment, D2 (moderate): structural damage and moderate non-structural damage, D3 (significant): heavy structural damage, D4 (near collapse): extensive wall damage and partial roof and floor failure, D5 (collapse): the complete collapse of structural and non-structural elements. The damage distribution is illustrated using the DPM as reported in [Figure 11](#).

The main overcome indicates a significant increase in building vulnerability passing from intensity V to XII. For example, at intensity X, the prevailing damage state for a 500-year return period is D3 (significant), affecting 170 buildings. At intensity XI, the dominant damage state shifts to D4 (near collapse), affecting nearly 200 buildings. This vulnerability continues at intensity XII, where D4 (near collapse) and D5 (collapse) damage states are observed in 150 and 105 buildings, respectively. To elucidate the behavior of seismic intensity, the study employs probability estimates of collapse and unusability based on the conceptual frameworks introduced by Bramerini *et al.*^[31] and subsequently used by Servizio Sismico Nazionale (SSN)^[55]. The SSN approach incorporates multiplier factors ranging from 0 to 1. These formulas provide empirical equations aimed at determining the probabilistic percentages of collapsed and unusable buildings, as well as human casualties and individuals rendered homeless^[55]. Probabilities of collapse, death, and homelessness are plotted against each intensity class to describe the behavior of buildings under various earthquake intensities [[Figure 12](#)]. These probabilities are calculated as follows:

$$P(\text{collapse}) = P(D5) \quad (10)$$

$$P(\text{homeless}) = P(D3) \times w_{ei,3} + P(D4) \times w_{ei,4} \quad (11)$$

$$P(\text{dead}) = 0.3 \times P(D5) \quad (12)$$

$$P(\text{homeless}) = P(D3) \times w_{ei,3} + P(D4) \times w_{ei,4} + 0.7 \times P(D5) \quad (13)$$

The multiply factors $w_{ei,3} = 0.4$ and $w_{ei,4} = 0.6$ are as reported in^[56].

[Table 4](#) and [Figure 12](#) illustrate a direct correlation between earthquake intensity and the probability of building collapse. Notably, beyond a certain intensity level, i.e., X grade, the probability of buildings becoming unusable starts to decrease. This anomaly can be attributed to the fact that some structures initially assigned a D3 grade have already collapsed, leading to a decrease in the probability of unusable buildings.

Table 4. Probabilities of homelessness; unusable; collapse; and death for different intensities

Intensity	$P_{hom.}$ (%)	$P_{un.}$ (%)	$P_{coll.}$ (%)	P_{dead} (%)
IX	4.0	4.0	-	-
X	33	33	-	-
XI	55	53	2.0	1
XII	64	35	40	12

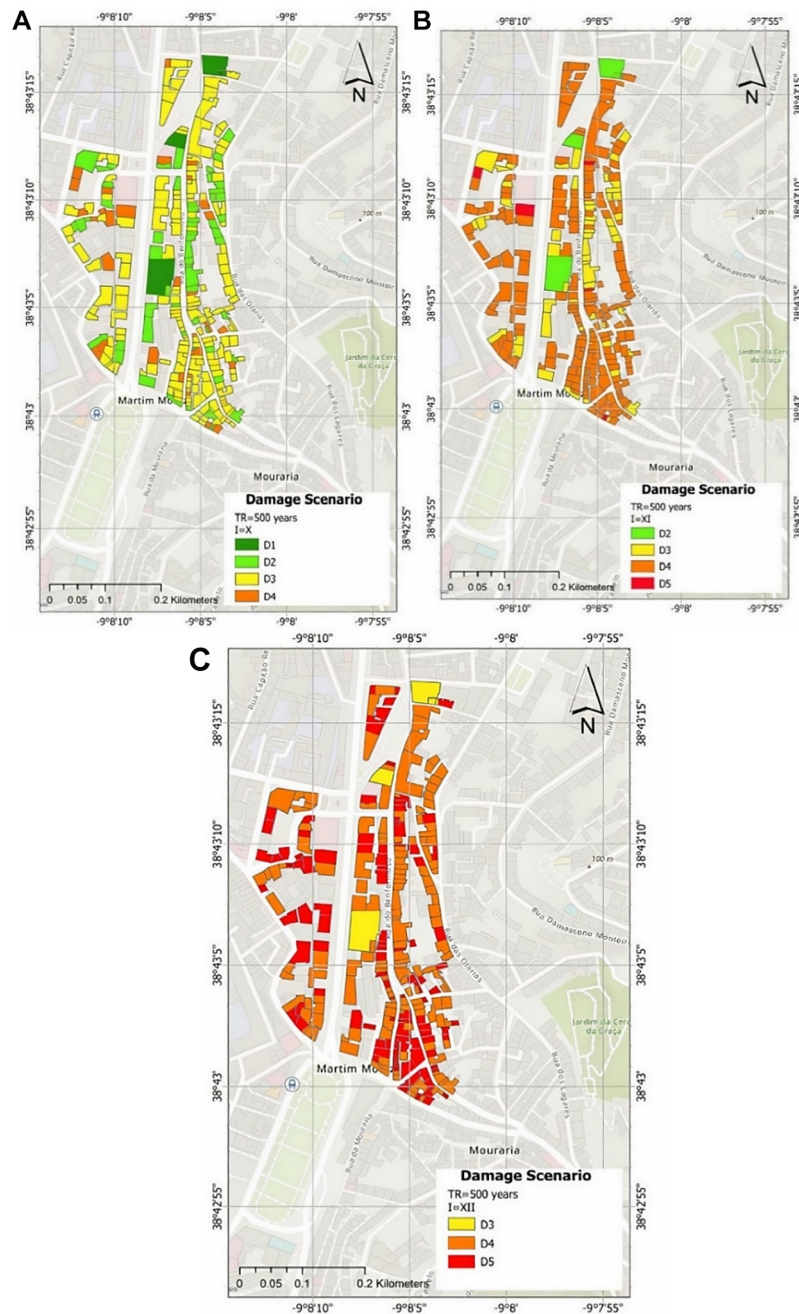


Figure 11. Damage scenarios for the estimated intensities: (A) X grade; (B) XI grade; and (C) XII grade with a 500-year return period.

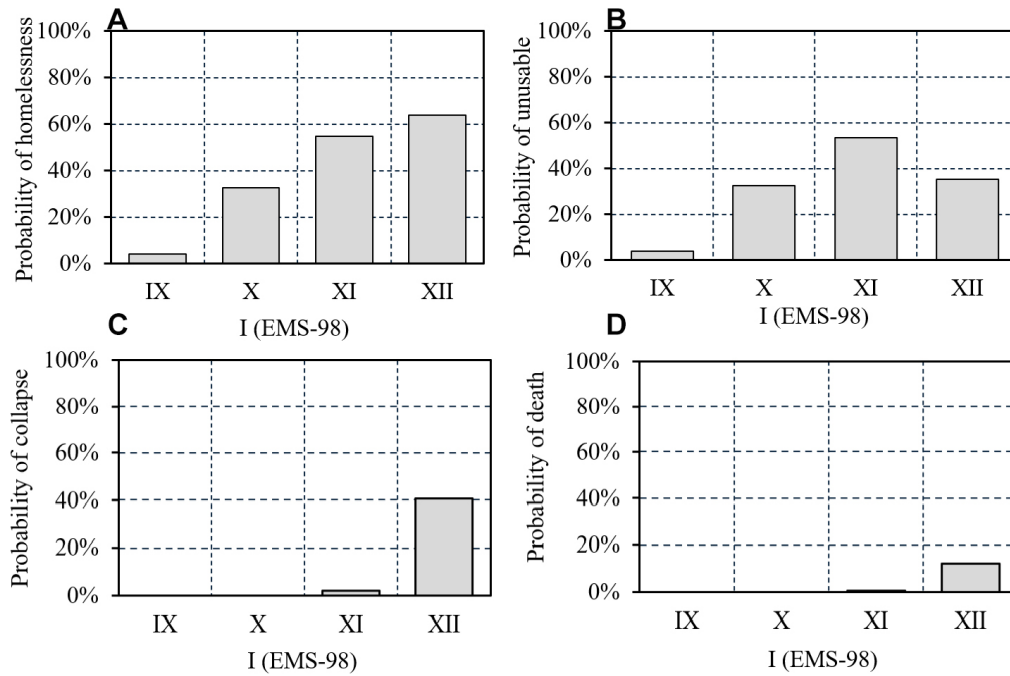


Figure 12. Probabilities of (A) Homelessness; (B) Unusable; (C) Collapse; and (D) Death.

LOSS ESTIMATION

The seismic vulnerability assessment of historic urban centers involves economic loss and repair cost estimation, crucial for understanding the risk associated with seismic events. A quantitative approach evaluates the replacement cost of damaged buildings, considering factors such as retrofitting expenses. The comprehensive approach includes building inventory, damage assessment, and cost estimation, with a standardized cost of 1,500 euros per square meter for restoring historic buildings. This amount is based on Lantada's study conducted in 2018^[54] and has been adjusted for inflation and validated through recent on-site surveys to ensure it reflects current market conditions. As a standardized metric, it serves as a valuable reference point for guiding risk management and mitigation strategies for historic structures.

The cost of retrofitting damaged buildings depends on the level of degradation, with damage grades contributing to varying degrees of building deterioration, thereby influencing economic loss. For a building (j) of type (t), the probability of economic repair costs is determined by parameters such as the unit cost (Vc_t) per square meter of damaged area, which is assumed constant across buildings of the same type. The evaluation model for repair and replacement costs involves calculating the building area ($Area_{jt}$) in square meters, multiplying it by the probability of each damage state (P_{jtk}) and the corresponding repair cost (RC_{tk}). Summing over all damage states yields the total repair cost for a single building. This model is then applied to all buildings of each type across the population, resulting in a comprehensive model for estimating economic loss and repair costs^[54].

$$cost = \sum_{t=1}^{Nt} \left\{ Vc_t \sum_{j=1}^{Net} \left[Area_{jt} \sum_{k=1}^{Ns} P_{jtk} \cdot RC_{tk} \right] \right\} \quad (14)$$

The repair cost (RC_{ik}) for a specific building type is expressed as a percentage of the unit cost per square meter. The probability of each damage state (P_{jik}) is derived from a damage probability matrix. Calculations include the number of non-null damage states N_s , building area ($Area_{jt}$), and estimated cost (Vc_i), based on material and labor expenses for restoration, excluding land costs. N_{et} represents the total buildings of type t , and N_i is the number of building types. The total repair costs in the range of millions for different intensities are illustrated in [Figure 13](#), indicating negligible costs for the first two intensities, near zero. Then, they rise to 9 and 10 million for intensities VIII and IX, respectively. Consequently, they soar significantly for intensities XI and XII, reaching 23 and 25 million.

Moreover, in terms of thousands of euros, individual building costs are presented in [Figure 14](#) for the lowest and highest intensities, V and XII. These graphs reveal that the costs per building are notably low for the initial intensities, nearly zero for intensity V, as shown in [Figure 14A](#). However, as the intensity increases, the cost for each building experiences a substantial surge. Notably in [Figure 14B](#), by intensity XII, the costs reach their peak, with almost every building requiring extensive funds for repair and renovation.

The repair costs per building are calculated in the same manner as the total repair cost, using the same equation and parameters. The variable V_i , which is the horizontal axis, represents a feature belonging to each building according to its vulnerability index derived from Equation 3. For instance, a building with a V_i of 0.6 at intensity XII needs around 1,200 thousand euros for repair costs. This is because this specific building has a vulnerable typology, which is Pombalino, and a damage grade of 5 for intensity XII. Additionally, its large plan area of 1,700 square meters contributes to it being the most vulnerable and expensive house to repair at intensity XII.

RESILIENCE INDEX

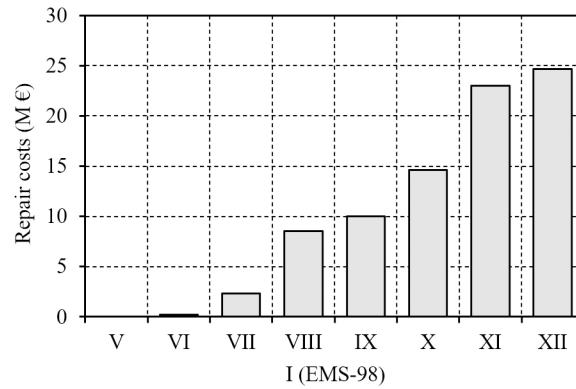
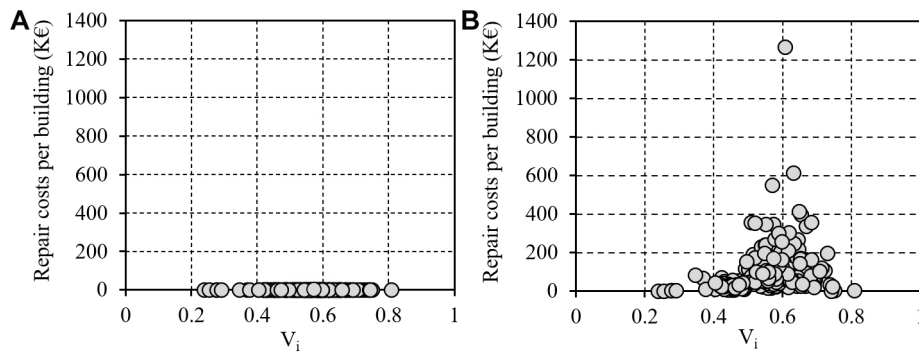
The resilience index serves as a metric to gauge a system's ability to swiftly return to normal operations in the aftermath of a disaster.

In the realm of post-disaster management, particularly in the context of community recovery following significant earthquakes, assessing system performance becomes pivotal. Utilizing resilience as a foundational principle can effectively inform decisions aimed at enhancing the performance of structures and infrastructures during extreme events. The recovery period, a critical aspect of post-disaster management, is heavily influenced by the availability of economic resources, and it profoundly influences community resilience. The duration of recovery is contingent upon socioeconomic factors and the methodologies employed in political decision-making. Nations that have experienced major earthquakes have adopted diverse disaster management models, with the reconstruction of entirely damaged buildings often spanning multiple years. This study evaluates the resilience index based on recovery time, a variable dependent on the severity of building damages. A recovery time coefficient, denoted as C_r , is derived to quantify the degree of damage. This coefficient represents the ratio of a structure's total reconstruction time to the time required for partial repair. Additionally, repair costs play a pivotal role in community resilience, as the extent of damage to buildings directly influences them. The study delves into repair cost details; specifically, the anticipated Cost Ratio, C_c , needed to address a specific damage state. C_c is defined as the ratio of the total building replacement cost to the cost of partial repairs.

All building types, including Masonry, Reinforced Concrete, and Steel structures, are considered in the proposed building resilience index. Resilience, in this context, is quantified by a structure's capacity to function post-earthquake, with three key factors underpinning this assessment: damage level (dependent on the seismic intensity and vulnerability index), recovery duration, and recovery cost^[57], as shown in [Table 5](#).

Table 5. Time recovery and cost recovery factors

Damage level (μ_D)	Time Recovery factor (C_t)	Cost Recovery factor (C_c)
1	0.03	0.04
2	0.20	0.22
3	0.38	0.43
4	0.42	0.49
5	1.00	1.00

**Figure 13.** Total repair costs of the examined buildings for different intensities.**Figure 14.** Repair costs per building for intensities of V (A) and XII (B).

$$RI = 1 - (\mu_D \times C_t \times C_c) \quad (15)$$

The results, as depicted in [Figure 15](#), focus on the lowest and highest intensities as they represent critical points in understanding the resilience of buildings. At lower intensities, i.e., intensity V, buildings exhibit 100% resilience, showcasing their ability for reuse even after experiencing seismic activity (see [Figure 15A](#)).

However, as intensities increase, resilience indices gradually decrease. By intensities IX and X, most buildings are only 50% usable, indicating a significant decline in their resilience. Finally, at the highest intensities, depicted by intensities XI and XII, resilience indices drop to zero, highlighting the critical need for conservation and interventions as the buildings become completely unusable as reported in [Figure 15B](#).

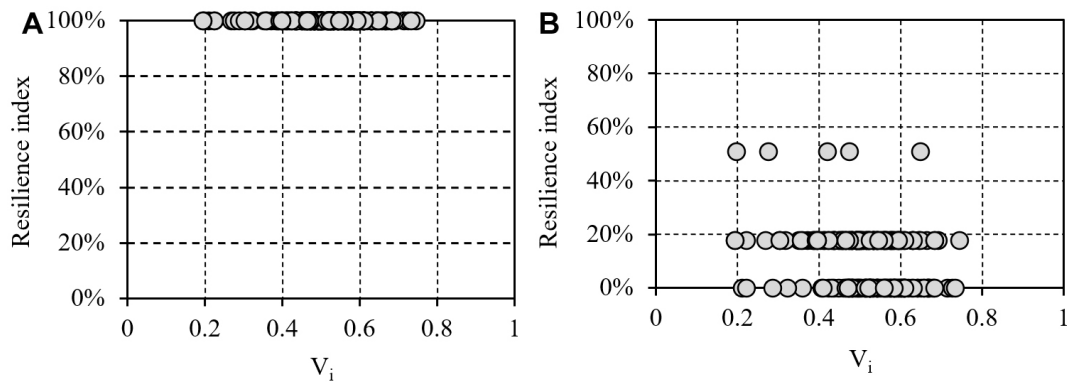


Figure 15. Resilience indices for intensities of (A) a scenario for intensity V and (B) a scenario for intensity XII.

STRENGTHENING SOLUTIONS AND RECOMMENDATIONS

To reduce the vulnerability of the analyzed building sample, several retrofitting interventions have been implemented to improve the seismic capacity of the investigated compound. These interventions include enhancing orthogonal connections, i.e., wall-to-wall and wall-to-floor/roof diaphragm connections, enhancing the in-plane strength of horizontal diaphragms, strengthening exterior structural elements and reinforcing or constraining walls, all of which were highlighted as feasible solutions. After these upgrades, the parameters used to calculate vulnerability indices were re-evaluated to reflect the overall improvements. The adopted strengthening interventions were simulated to evaluate their effectiveness, and input into Python codes by upgrading the corresponding vulnerability parameters of the above-introduced survey form (see Section "Index-based vulnerability approach"). In this context, the normalized vulnerability index was recorded for each typology and four notably vulnerable buildings. Detailed results of the iterative strengthening can be found in Table 6, and Figure 16 provides an overview of the general reduction in repair costs per million after the application of the retrofitting of the buildings.

According to Table 6, for the M1, M5, and M6 typologies, enhancing orthogonal wall-to-wall connections and a combination of wall-to-wall and floor-to-wall improvements had the most significant impact, resulting in up to a 16% improvement. Particularly for the M7 typology, grouted stitching stones, structural repointing, and lime injection proved effective, improving by approximately 21%. However, their implementation comes with a significant cost, and the irreversible nature of these methods should be taken into account. A similar pattern is observed for the four notably vulnerable buildings.

On the other hand, Figure 16 illustrates the repair costs per million for both post and ante-interventions and strengthening. According to the graph, it is obvious that the repair costs decreased after interventions, with the most significant decline occurring at intensity XII, where the total costs dropped from 25 to 16 million.

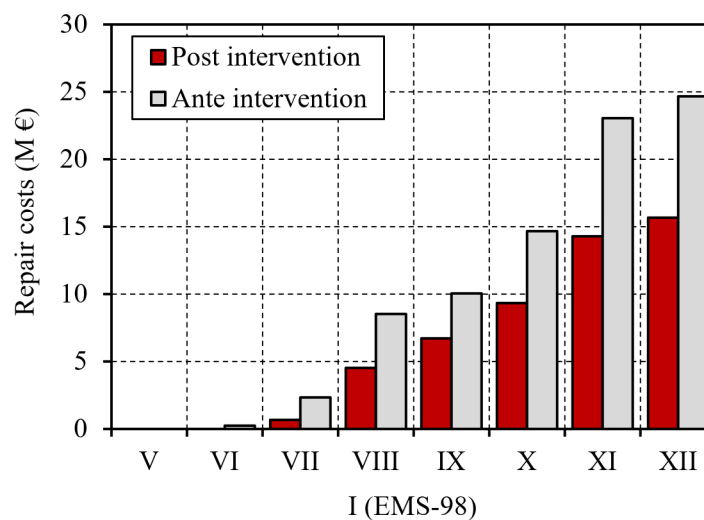
CONCLUSION

This study, which focused on the seismic vulnerability of the historic center of Lisbon, Portugal, underscores the critical need for proactive risk reduction in earthquake-prone regions with aging building stock.

Drawing from lessons learned from catastrophic earthquakes globally and recognizing the enduring consequences of seismic events on human life, economic stability, and heritage preservation, the research contributes to the broader discourse on mitigating seismic risk.

Table 6. Effectiveness of strengthening methods: normalized vulnerability index results for different building typologies

Typology/Building	V_i							
	<i>In-situ</i>	Exterior upgrades	Wall-wall connections	Floor-wall connections	Both wall-wall and floor-wall connections	Floor connections and stiffening	Roof tie addition	Lime injection and repointing
M1: Pre/Pombaline	0.57	0.56	0.51	0.55	0.51	0.52	0.53	0.54
		1.75%	10.53%	3.51%	10.53%	8.77%	7.02%	5.26%
M5: Gaioleiro	0.54	0.53	0.48	0.51	0.45	0.48	0.5	0.47
		1.85%	11.11%	5.56%	16.67%	11.11%	7.41%	12.96%
M6: Placa	0.49	0.48	0.44	0.47	0.4	0.47	0.48	0.41
		2.04%	10.20%	4.08%	18.37%	4.08%	2.04%	16.33%
M7: RCM	0.43	0.43	0.43	0.43	0.39	0.43	0.43	0.34
		0.00%	0.00%	0.00%	9.30%	0.00%	0.00%	20.93%
Bldg 1: Gaioleiro	0.81	0.79	0.77	0.78	0.69	0.75	0.74	0.64
		2.30%	4.77%	3.54%	14.67%	7.25%	8.48%	20.85%
Bldg 47: Pombalino	0.73	0.72	0.69	0.71	0.61	0.68	0.69	0.66
		1.37%	5.48%	2.74%	16.44%	6.85%	5.48%	9.59%
Bldg 262: Pombalino	0.745	0.72	0.7	0.745	0.65	0.71	0.72	0.67
		3.36%	6.04%	0.00%	12.75%	4.70%	3.36%	10.07%
Bldg 277: Placa	0.617	0.617	0.57	0.56	0.49	0.56	0.59	0.52
		0.00%	7.62%	9.24%	20.58%	9.24%	4.38%	15.72%

**Figure 16.** Impact of retrofitting on repair costs per million for strengthened buildings.

The challenges in seismic evaluations, including time and cost constraints, emphasize the importance of territorial seismic vulnerability assessments with detailed information on the building structure, materials and construction practices for accurate risk assessment. The statistical approaches, vulnerability and fragility curves, and predicted damage scenarios offer a comprehensive framework for assessing and understanding seismic risks. The focus on masonry residential buildings, a prevalent and vulnerable construction style, enhances the applicability of the findings. Beyond structural assessments, the study extends to economic implications, estimating repair costs, and presenting a resilience index to gauge the current condition of buildings. Collaborating with the ReSist Program, the research aligns with ongoing municipal initiatives for seismic vulnerability assessment. By integrating a large-scale vulnerability assessment methodology, the

project complements the program's objectives and offers intervention recommendations and strengthening solutions. The holistic approach presented advocates for the incorporation of comprehensive risk assessment methodologies in urban management practices. As seismic events continue to pose a significant threat to historic city centers, the study highlights the importance of adopting and implementing technical standards for assessing seismic vulnerability. The ReSist Program, with its components of management plans, educational campaigns, site inspections, and criteria for prioritizing interventions, serves as a model for other regions aiming to enhance their resilience to seismic risks.

In conclusion, the research contributes valuable insights and practical recommendations for addressing seismic vulnerability in historic city centers. It is hoped that the findings presented will guide future efforts in urban planning, seismic risk reduction, and heritage preservation, ultimately fostering resilient and sustainable communities in seismic-prone areas. Future endeavors should focus on expanding datasets, integrating socio-cultural factors, employing advanced modeling techniques, implementing long-term monitoring strategies, engaging communities, strengthening policies, and fostering interdisciplinary collaboration. By addressing these areas, efforts can be enhanced in urban planning, seismic risk reduction, and heritage preservation, ultimately fostering resilient and sustainable communities in seismic-prone areas.

In comparison with similar studies conducted by Xofi *et al.*^[58] and Barchetta *et al.*^[59], both of which investigated the metropolitan area of Lisbon, the current research aligns with its commitment to developing effective and scalable seismic vulnerability assessment methodologies for urban centers. The study by Xofi demonstrates the benefit of simplified, index-based approaches to quickly identify vulnerable areas using census data, offering insights into urban seismic risk on a large scale. By combining vulnerability results with hazard levels, the methodology by Xofi effectively supports prioritization for risk management, though it is limited by data granularity and suggests the need for on-site verification to enhance accuracy. Similarly, the research by Barchetta underscores the effectiveness of rapid resilience assessments for historic centers, employing a geodatabase to visualize and interpret risk distribution. However, it highlights the limitations inherent in assessing modified historic structures, where undocumented alterations may impact seismic vulnerability. The current study builds on these approaches by proposing a resilience index and by directly comparing results with on-site surveys, ensuring that findings not only reflect local vulnerabilities but also contribute to actionable municipal policies.

Rapid visual screening (RVS) methods, developed by Purushothama^[60], enable preliminary assessments of building vulnerability without detailed modeling, making them particularly useful in high-seismicity areas with structures lacking seismic design. While RVS provides a safety index from visual inspections, its accuracy can be influenced by unmeasured building features. To enhance RVS effectiveness, future work should focus on improving data quality and integrating comprehensive evaluations for better vulnerability assessment and intervention strategies for historic city centers.

This comparative discussion reinforces the importance of enhancing data quality and integrating comprehensive, on-the-ground evaluations to refine vulnerability assessment models and improve intervention strategies for historic city centers, especially in Portugal.

DECLARATIONS

Acknowledgments

Amaral Ferreira M expresses gratitude for the funding provided by the Foundation for Science and Technology. Amaral Ferreira M and Oliveira CS are grateful for the support provided by the Foundation for Science and Technology through funding from the research unit CERIS.

Authors' contributions

Conceptualization, methodology, analysis and writing: Chieffo N, Mehralian H
Software coding and numerical analysis: Moritz M, Mehralian H, Gögen B, Khodadadi A
Supervision and review: Chieffo N, Amaral Ferreira M, Oliveira CS

Availability of data and materials

The functions were designed to utilize the Pandas data analysis library for efficient reading of Excel databases. The code is publicly available on github.com^[52], enabling users to conduct seismic vulnerability assessments of historic structures.

Financial support and sponsorship

The funding provided by the Foundation for Science and Technology (DOI:10.54499/CEECINST/00122/2018/CP1528/CT0025); The Foundation for Science and Technology through funding UIDB/04625/2020 from the research unit CERIS (DOI:10.54499/UIDB/04625/2020).

Conflicts of interest

All authors declared that there are no conflicts of interest.

Ethical Approval and Consent to Participate

Not applicable.

Consent for Publication

Not applicable.

Copyright

© The Author(s) 2024.

REFERENCES

1. Stellacci S, Rato V, Poletti E. Structural permanence in pre- and post-earthquake Lisbon: half-timbered walls in overhanging dwellings and in *Pombalino* buildings. *Int J Architect Herit* 2016;11:363-81. DOI
2. Bernardo V, Costa CA, Candeias P, Costa A, Lourenço P. Analytical seismic fragility curves for ancient masonry buildings in Portugal. Zagreb, Croatia; 2023. DOI
3. Margesson R, Taft-Morales M. Haiti earthquake: crisis and response. 2010. Available from: https://www.everycrsreport.com/files/20100308_R41023_ef960f2289f3fff5c83e5c956e08a84e9f45f747.pdf [Last accessed on 26 Nov 2024].
4. Ritsema J, Lay T, Kanamori H. The 2011 Tohoku Earthquake. *Elements* 2012;8:183-8. DOI
5. Mavrouli M, Mavroulis S, Lekkas E, Tsakris A. An emerging health crisis in Turkey and Syria after the earthquake disaster on 6 february 2023: risk factors, prevention and management of infectious diseases. *Healthcare* 2023;11:1022. DOI PubMed PMC
6. John EH. Disaster risk reduction and climate change adaptation in the Pacific: an institutional and policy analysis; 2012. Available from: <https://www.undrr.org/publication/disaster-risk-reduction-and-climate-change-adaptation-pacific-institutional-and-policy> [Last accessed on 28 Nov 2024].
7. Calvi GM, Pinho R, Magenes G, Bommer JJ, Restrepo-Vélez LF, Crowley H. Development of seismic vulnerability assessment methodologies over the past 30 years. *ASET J Earthq Technol* 2006;43:75-104. Available from: https://www.researchgate.net/publication/241826044_Development_of_seismic_vulnerability_assessment_methodologies_over_the_past_30_years [Last accessed on 26 Nov 2024]
8. Ahmed S, Abarca A, Perrone D, Monteiro R. Large-scale seismic assessment of RC buildings through rapid visual screening. *Int J Disaster Risk Reduct* 2022;80:103219. DOI
9. Aguado JLP, Ferreira TM, Lourenço PB. The use of a large-scale seismic vulnerability assessment approach for masonry façade walls as an effective tool for evaluating, managing and mitigating seismic risk in historical centers. *Int J Architect Herit* 2018;12:1259-75. DOI
10. Formisano A, Florio G, Landolfo R, Mazzolani FM. Numerical calibration of an easy method for seismic behaviour assessment on large scale of masonry building aggregates. *Adv Eng Softw* 2015;80:116-38. DOI
11. Mehralian H, Azarbakht A. Seismic loss assessment: the case study of the power distribution network in Arak city, Iran. *J Civ Eng Mater Appl* 2020;4:195-207. DOI

12. Tatangelo M, Audisio L, D'Amato M, Gigliotti R. Issues related to typological fragility curves derivation starting from observed seismic damage. *Eng Struct* 2024;307:117853. DOI
13. Porter K, Kennedy R, Bachman R. Creating fragility functions for performance-based earthquake engineering. *Earthq Spectra* 2007;23:471-89. Available from: <https://www.sparisk.com/pubs/Porter-2007-deriving-fragility.pdf> [Last accessed on 26 Nov 2024]
14. Rota M, Penna A, Magenes G. A methodology for deriving analytical fragility curves for masonry buildings based on stochastic nonlinear analyses. *Eng Struct* 2010;32:1312-23. DOI
15. Vilanova SP, Fonseca JFBD. Probabilistic seismic-hazard assessment for Portugal. *Bull Seismol Soc Am* 2007;97:1702-17. DOI
16. Dynes RR. The Lisbon earthquake in 1755: the first modern disaster; 2003. Available from: <http://udspace.udel.edu/handle/19716/294> [Last accessed on 26 Nov 2024].
17. Oliveira CS. Historical seismicity and revision of the seismic catalogue. LNEC; 1986. (In portuguese)
18. Chester DK, Chester OK. The impact of eighteenth century earthquakes on the Algarve region, southern Portugal. *Geogr J* 2010;176:350-70. DOI
19. Silva V, Crowley H, Varum H, Pinho R. Seismic risk assessment for mainland Portugal. *Bull Earthq Eng* 2015;13:429-57. DOI
20. Statistics IN from census data. Lisbon; 2011. In Portuguese. Available from: https://www.ine.pt/xportal/xmain?xpid=INE&xpgid=ine_publicacoes&PUBLICACOESpub_boui=73212469&PUBLICACOESmodo=2 [Last accessed on 28 Nov 2024].
21. Simões AGG. Evaluation of the seismic vulnerability of the unreinforced masonry buildings constructed in the transition between the 19th and 20th centuries in Lisbon, Portugal; 2018. Available from: https://ceris.pt/wp-content/uploads/2024/05/2018_RG6_Rita-Bento-Ana-Simoes.pdf [Last accessed on 26 Nov 2024].
22. Erberik MA. Generation of fragility curves for Turkish masonry buildings considering in-plane failure modes. *Earthq Engng Struct Dyn* 2008;37:387-405. DOI
23. Borzi B, Crowley H, Pinho R. Simplified pushover-based earthquake loss assessment (SP-BELA) method for masonry buildings. *Int J Architect Herit* 2008;2:353-76. DOI
24. Costa AC, Sousa ML, Carvalho A, Coelho E. Evaluation of seismic risk and mitigation strategies for the existing building stock: application of LNECloss to the metropolitan area of Lisbon. *Bull Earthq Eng* 2010;8:119-34. DOI
25. Milosevic J, Bento R, Cattari S. Seismic behavior of Lisbon mixed masonry-RC buildings with historical value: a contribution for the practical assessment. *Front Built Environ* 2018;4:43. DOI
26. Simões A, Milošević J, Meireles H, Bento R, Cattari S, Lagomarsino S. Fragility curves for old masonry building types in Lisbon. *Bull Earthq Eng* 2015;13:3083-105. DOI
27. Mosoarca M, Onescu I, Onescu E, Anastasiadis A. Seismic vulnerability assessment methodology for historic masonry buildings in the near-field areas. *Eng Fail Anal* 2020;115:104662. DOI
28. Lagomarsino S. On the vulnerability assessment of monumental buildings. *Bull Earthq Eng* 2006;4:445-63. DOI
29. Lagomarsino S, Cattari S, Ottonelli D. The heuristic vulnerability model: fragility curves for masonry buildings. *Bull Earthq Eng* 2021;19:3129-63. DOI
30. Chieffo N, Formisano A, Landolfo R, Milani G. A vulnerability index based-approach for the historical centre of the city of Latronico (Potenza, Southern Italy). *Eng Fail Anal* 2022;136:106207. DOI
31. Brammerini F, Castenetto S, Cubellis E, Martini MG, Rebuffat M, Soddu P. Earthquake, GIS and multimedia. The 1883 Casamicciola earthquake. 1995. Available from: <http://hdl.handle.net/2122/1798> [Last accessed on 26 Nov 2024].
32. ReSist. Informações E Serviços. Câmara Municipal de Lisboa; 2023. Available from: <https://informacoeseservicos.lisboa.pt/prevencao/resiliencia-urbana/projetos/resist> [Last accessed on 26 Nov 2024].
33. Pinto C, Ferreira MA, Pacheco P, et al. The resist programme: Lisbon strategy for seismic resilience. In 18th World Conference on Earthquake Engineering (WCEE2024), 30 June-5 July 2024; Milan, Italy. Available from: https://www.researchgate.net/publication/382159159_THE_RESIST_PROGRAMME_LISBON_STRATEGY_FOR_SEISMIC_RESILIENCE [Last accessed on 26 Nov 2024].
34. Oliveira CS, Lopes M, Mota de Sá F, et al. New steps towards a simple model of the building stock and corresponding seismic vulnerabilities: situations of great similarity of buildings and cases of poor consistency. In 18th World Conference on Earthquake Engineering (WCEE2024), 30 June-5 July 2024; Milan, Italy. Available from: https://www.researchgate.net/publication/382160580_New_steps_towards_a_simple_model_of_the_building_stock_and_corresponding_seismic_vulnerabilities_Situations_of_great_similarity_of_buildings_and_cases_of_poor_consistency [Last accessed on 30 Nov 2024].
35. MOREIRA VS. Seismicity of the Portuguese continental margin. 1989; pp. 533-45. Available from: <http://pascal-francis.inist.fr/vibad/index.php?action=getRecordDetail&idt=7229218> [Last accessed on 26 Nov 2024].
36. Lisboa AMD. Mapa das freguesias de Lisboa; 2022. Available from: <https://www.am-lisboa.pt/451600/1/009001,000531/index.htm> [Last accessed on 26 Nov 2024].
37. Sá L, Morales-Esteban A, Durand Neyra P. The 1531 earthquake revisited: loss estimation in a historical perspective. *Bull Earthq Eng* 2018;16:4533-59. DOI
38. Teves-Costa P, Batlló J, Matias L, Catita C, Jiménez MJ, García-Fernández M. Maximum intensity maps (MIM) for Portugal mainland. *J Seismol* 2019;23:417-40. DOI
39. Gögen B, Karimzadeh S, Lourenço PB. Probabilistic seismic hazard assessment of Lisbon (Portugal). *GeoHazards* 2024;5:932-70. DOI
40. Ferrão C, Bezzeghoud M, Caldeira B, Borges JF. The seismicity of Portugal and its adjacent atlantic region from 1300 to 2014: maximum observed intensity (MOI) map. *Seismol Res Lett* 2016;87:743-50. DOI

41. Araãjo AC. The 1755 Lisbon earthquake: the catastrophe and the reconstruction. *Storicamente* 2021;17. DOI
42. Google Earth. Available from: <https://earth.google.com> [Last accessed on 26 Nov 2024].
43. Environmental Systems Research Institute. ArcGIS version 10.8.1; 2020. Available from: <https://www.arcgis.com/index.html> [Last accessed on 28 Nov 2024].
44. Bernardo V, Sousa R, Candeias P, Costa A, Campos Costa A. Historic appraisal review and geometric characterization of old masonry buildings in Lisbon for seismic risk assessment. *Int J Archit Herit* 2022;16:1921-41. DOI
45. Grunthal G. European macroseismic scale. Centre Européen de Géodynamique et de Séismologie; 1998. Available from: https://media.gfz-potsdam.de/gfz/sec26/resources/documents/PDF/EMS-98_Original_englisch.pdf [Last accessed on 28 Nov 2024].
46. Formisano A. Theoretical and numerical seismic analysis of masonry building aggregates: case studies in San Pio Delle Camere (L'Aquila, Italy). *J Earthq Eng* 2017;21:227-45. DOI
47. Basaglia A, Cianchino G, Cocco G, et al. An automatic procedure for deriving building portfolios using the Italian "CARTIS" online database. *Structures* 2021;34:2974-86. DOI
48. Mosoarca M, Onescu I, Onescu E, Azap B, Chieffo N, Szitar-Sirbu M. Seismic vulnerability assessment for the historical areas of the Timisoara city, Romania. *Eng Fail Anal* 2019;101:86-112. DOI
49. Vicente R, Parodi S, Lagomarsino S, Varum H, Silva JARM. Seismic vulnerability and risk assessment: case study of the historic city centre of Coimbra, Portugal. *Bull Earthq Eng* 2011;9:1067-96. DOI
50. Chieffo N, Formisano A, Lourenço PB. Seismic vulnerability procedures for historical masonry structural aggregates: analysis of the historical centre of Castelpoto (South Italy). *Structures* 2023;48:852-66. DOI
51. Python programming Language. Version 3.6.8. Python software foundation. Available from: <http://www.python.org/> [Last accessed on 26 Nov 2024].
52. Moritz M. Vulnerability-index-method. GitHub; 2023. Available from: <https://github.com/masonmoritz/Vulnerability-Index-Method-SAHC> [Last accessed on 26 Nov 2024].
53. Oliveira CS. Lisbon earthquake scenarios: a review on uncertainties, from earthquake source to vulnerability modelling. *Soil Dyn Earthq Eng* 2008;28:890-913. DOI
54. Lantada N, Pujades LG, Barbat AH. Earthquake risk scenarios in urban areas: a review with applications to the Ciutat Vella district in Barcelona, Spain. *Int J Architect Herit* 2018;12:1112-30. DOI
55. Lucantoni A, Bosi V, Brammerini F, et al. Seismic risk in Italy (In Italian). *Ingegneria Sismica*; 2001, pp. 5-36. Available from: https://www.researchgate.net/publication/313419051_Seismic_risk_in_Italy [Last accessed on 30 Nov 2024]
56. Vicente R, Ferreira T, Maio R. Seismic risk at the urban scale: assessment, mapping and planning. *Proc Econ Financ* 2014;18:71-80. DOI
57. Yousfi N, Mounir AB, Boukri M, Guessoum N, Bensaibi M. Seismic resilience assessment of buildings: case study of Blida city; 2022. Available from: <https://www.researchsquare.com/article/rs-2137910/v1> [Last accessed on 26 Nov 2024].
58. Xofi M, Ferreira TM, Domingues JC, et al. On the seismic vulnerability assessment of urban areas using census data: the Lisbon metropolitan area as a pilot study area. *J Earthq Eng* 2024;28:242-65. DOI
59. Barchetta L, Petrucci E, Xavier V, Bento R. A simplified framework for historic cities to define strategies aimed at implementing resilience skills: the case of Lisbon downtown. *Buildings* 2023;13:130. DOI
60. Purushothama C, Mucedero G, Perrone D, Monteiro R. Evaluation of rapid visual screening assessment of existing buildings using nonlinear numerical analysis. *J Build Eng* 2023;76:107110. DOI